

## A COMPARATIVE STUDY BETWEEN WEIGHING AND IMAGE ANALYSIS TECHNIQUES FOR PREDICTING THE AMOUNT OF DEPOSITED ELECTROSPUN NANOFIBRES

A.H. Nurfaizey<sup>1</sup>, F.C. Long<sup>1</sup>, M.A.M. Daud<sup>1</sup>, N. Muhammad<sup>1</sup>,  
N.A. Masripan<sup>1</sup> and N. Tucker<sup>2</sup>

<sup>1</sup>Faculty of Mechanical Engineering,  
Universiti Teknikal Malaysia Melaka, Hang Tuah Jaya, 76100 Durian  
Tunggal, Melaka, Malaysia.

<sup>2</sup>University of Lincoln, Brayford Pool, Lincoln,  
LND 7TS, United Kingdom.

Corresponding Author's Email: [nurfaizey@utem.edu.my](mailto:nurfaizey@utem.edu.my)

**Article History:** Received 4 September 2018; Revised 6 July 2019;  
Accepted 2 October 2020

**ABSTRACT:** Weighing and direct measurement are currently the two most common techniques used for estimating the amount of deposited nanofibres in electrospinning process. Nevertheless, due to its extremely small fibre size and mass, the task of measuring the weight or thickness of an electrospun nanofibres membrane is difficult and the results are arguable. This study evaluates the effectiveness of using greyscale image analysis for predicting the amount of deposited nanofibres compared to weighing technique. Polyvinyl alcohol electrospun nanofibres were collected at different deposition times on A4 black paper substrates. The substrates were weighed before and after deposition process and then scanned into 8 bit greyscale images. Analyses were carried out using ImageJ software, statistical analysis, high speed camera and scanning electron microscopy. At long deposition times, both techniques showed significant correlations between the measured values and deposition times. However, at short deposition times the weighing technique was found unreliable ( $p > 0.05$ ) compared to image analysis technique due to insignificant fibre masses compared to the weight variation of the substrates. Results suggest that image analysis technique was a better option to be used compared to weighing technique. This technique has the potential to be used as an automated online quality control in electrospun nanofibres manufacture.

**KEYWORDS:** *Electrospinning; Electrospun Nanofibres; Greyscale; Image Analysis*

### 1.0 INTRODUCTION

Electrospinning is a straight forward process for producing polymeric nanofibres either from polymer solution or melt [1-3] with the presence of electrostatic forces. Even though a typical setup of an electrospinning process is simple, but the actual science underpinning the process is rather complicated [4]. When a high electric potential is applied to a pendant drop of a polymer solution, it will distribute throughout the solution and causes the charges to accumulate on the surface of the droplet.

Since like charges repel each other, the accumulation of the charges is accompanied by strong repulsive electric forces. When the electric forces overcome the surface tension of the droplet, the surface ruptures, and a charged jet of polymer is ejected from the droplet (Figure 1). At an equilibrium, the point of rupture forms a conical shape known as the Taylor cone [5]. The jet initially moves in a straight trajectory before it starts to buckle and continues the journey in an expanding helical path. Along the journey, solvent evaporation and fibre thinning continue until the fibres landed on the collector as random!

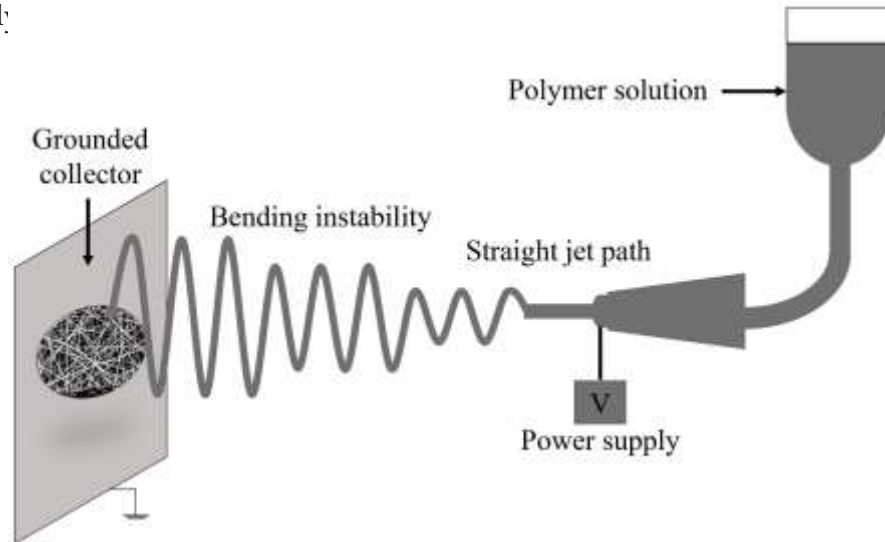


Figure 1: Schematic diagram of electrospinning process

Due to its extremely small fibre size and mass, electrospun nanofibres membranes exhibit unique properties such as high surface area to volume ratio, high porosity with small pore sizes, and lightweight [3, 6, 8]. These attributes make them highly potential as candidate for various applications including filtrations, sensors, protective clothing, and tissue engineering scaffolds [9-11]. However, small fibre size and lightweight make it difficult to quantify the actual amount of deposited electrospun nanofibres. Several attempts have been made to measure the thickness of the electrospun fibres such as the direct measurement using a micrometer [12], scanning electron microscopy (SEM) micrographs analysis [13] and light profilometry [14].

A micrometer provides a quick and easy method for measuring the thickness of any material. However, it requires a direct contact with the samples. Therefore, measuring the thickness of an electrospun nanofibres membrane using a micrometer would highly likely to cause the porous structure of the membrane to be compacted once a direct contact was applied onto the surface [12]. Using SEM micrographs or light profilometry technique to analyze the thickness of electrospun nanofibres membrane is a very time-consuming process. The measurements obtained are questionable due to the small sampling area compared to the actual size of the membrane. Furthermore, the cutting and handling processes during sample preparation can cause sample distortion [13-14]. Another popular option to estimate the amount of deposited electrospun nanofibres is

by using weighing technique. Stanger et al. [15] conducted an experiment to investigate the relationship between mass deposition rate and the applied voltage. The masses of the deposited fibres were found proportional to the deposition time. However, the measurement of the deposited fibres by using weighing method is rather challenging since the masses of the fibres were only in the range of a few micrograms compared to the weight of the substrates used in the experiment.

Image analysis is a non-destructive technique which has been used when characterizing electrospun nanofibres membranes. For instance, Ziabari et al. [16-17] used image analysis technique to automatically determine the fibre diameter of the nanofibrous structures at the intersection points. Ghasemi-Mobarakeh et al. [18] have successfully used image analysis method to measure the porosity of countless surface layers. Sambaer [19] proposed a 3D structure model of a polyurethane nanofibrous membrane based on image analysis method which will be used in filtration applications. A comparative study between an automated SEM image analysis and manual method in measuring fibre diameter has been conducted by Stanger et al. [20]. According to their studies, the main advantage of using automated image analysis technique is that it could analyze a large number of measurements in a short period of time.

The objective of this study is to investigate the feasibility of using greyscale image analysis method for predicting the amount of deposited electrospun nanofibres. A comparison between image analysis and weighing techniques has been carried out based on their ability to assess the different quantity of deposited fibres. A successful approach of this method has the potential to be used as an in-line non-destructive quality control method in electrospun fibre manufacturing.

## **2.0 METHODOLOGY**

Electrospun nanofibres were spun using poly(vinyl alcohol)(PVOH) with an average molecular weight of 124,000-130,000 g/mol and degree of hydrolysis (DH) in the range of 86-89% (Polyscientific, Malaysia). The PVOH was dissolved in distilled water with final concentration of 8 wt. %. The polymeric solution was stirred approximately for 2 hours at 60 °C using hot plate magnetic stirrer Model C-MAG HS7 (Ika Works, Malaysia).

The experimental work was conducted using a Model ES1a electrospinning machine (Electrospin Ltd., New Zealand). Axygen T-200-Y 200 µL pipette tip with an orifice diameter of 0.5 mm was used in this experiment. Black A4 papers were used as substrates to aid visibility. The substrates were weighed before and after sample collection using Model AG204 four figure balance (Mettler Toledo, Switzerland); with measurement error of ±0.0001g. Table 1 and Table 2 showed the samples of electrospun nanofibres collected at different deposition times with respective parameters. All the samples were left overnight to ensure that the solvent has fully evaporated.

All samples were scanned into 8-bit greyscale image using a commercial Canon Model MG5500 scanner. The scanning resolution was fixed at 300 dot per inch (dpi). ImageJ software (National Institutes of Health, NIH, USA) was used to measure the intensity value of each sample. Meanwhile, high speed camera Model Motion BLITZ Cube5 (Germany) was used to record the formation of the polymeric charged jet. The frame rate

of the camera was set at 3000 Hz. Samples of electrospun nanofibres were coated using platinum for 180 seconds using JEOL JEC-300FC auto fine coater whereas their morphological structure were observed under scanning electron microscopy (SEM) Model JEOL JSM-6010PLUS/LV. From the SEM micrographs, the average fibre diameter of the nanofibres was measured using ImageJ software and expressed in terms of mean  $\pm$  standard deviation (SD).

Table 1: Total samples produced at short deposition time with respective parameters

Short deposition time (s)	Time interval (s)	No. of sample	Total sample	Parameters		
				Voltage (kV)	Distance (cm)	Concentration (wt. %)
30-200	15,60	5	15	10	10	8

Table 2: Total samples produced at long deposition time with respective parameters

Long deposition time (s)	Time interval (s)	No. of sample	Total sample	Parameters		
				Voltage (kV)	Distance (cm)	Concentration (wt. %)
210-1800	60,120	17	51	10	10	8

### 3.0 RESULTS AND DISCUSSION

Figures 2 (a)-(d) show the formation of white circular spots of electrospun nanofibres at different deposition times. Out of 66 samples, four samples were used as examples as presented in Figures 2 (a)-(d). From visual observation, the size and intensity of the white spot for each sample increased as the deposition times increased. Surprisingly, a closer observation revealed there was a large amount of nanofibres accumulated at the centre of the circular spot. Based on this observation, it is safe to say that the nanofibre layer was denser at the centre compared to the edges of the circular spot. This finding was in agreement with the previous study conducted by Lee et al. [21]. In addition, the size of the circular spot seemed to be slightly increased as the deposition time increased. However, the size of the circular spot reached a maximum of approximately 7 cm in diameter determined by the size of electrospinning cone during electrospinning process.

Based on the scanned images from Figures 2 (a)-(d), a plot of surface topographic was produced by using ImageJ software Figures 2 (e)-(h)). The surface topographic plots resembled the formation of three-dimensional bell shape. The difference in the amount fibres among the samples were indicated by the height of the 3D plot. With reference to the scale bar, the height of the profile was observed to increase respectively with deposition time. The findings were consistent with the earlier observations, which proved that a large amount of nanofibres were located at the central area of the deposition area compared to the edges [21].

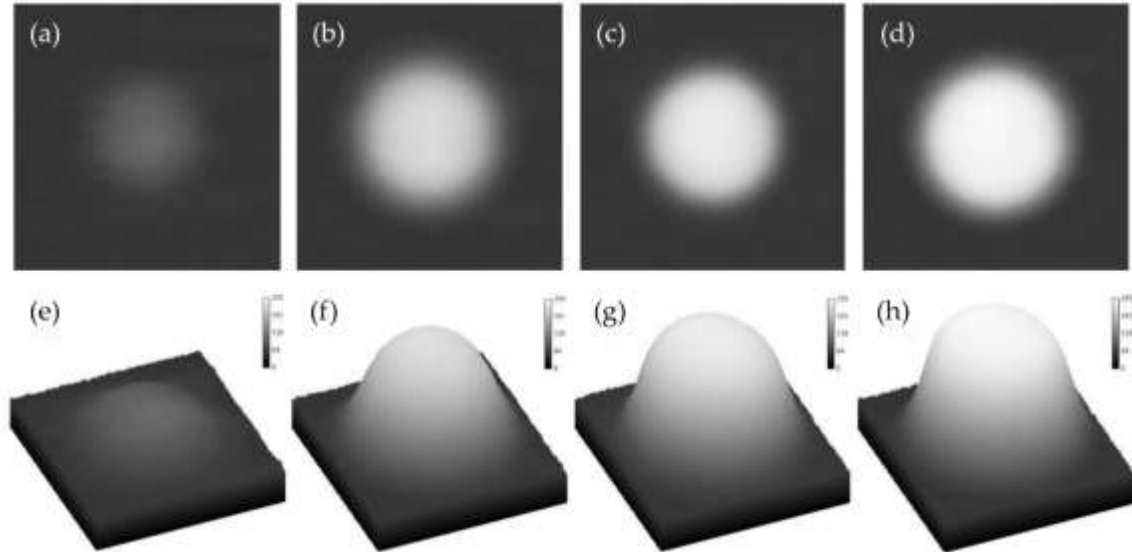


Figure 2: Deposited electrospun nanofibres collected at different deposition times: (a) 45s, (b) 600s, (c) 840s and (d) 1800s while subsequent topographic plots of greyscale intensities of the samples: (e) 45s, (f) 600s, (g) 840s and (h) 1800s

Previous studies by Reneker et al. [7] have described that bending instability occurred in a series of spiraling loops with increasing diameters as shown in Figure 3 (a). By analyzing the sample using ImageJ software, a sinusoidal curve image can be produced as presented in Figure 3 (b). However, the images obtained were not consistent with the results produced in Figures 2 (e)-(h). Thus, a high-speed camera was used to observe the formation of bending instability during the electrospinning process. Figure 4 (a) showed the actual bending instability as captured via high-speed camera and its subsequent schematic diagram shown in Figure 4 (b). It was observed that the movement of the nanofibres jet seemed to be in chaotic motion with most of the flying fibres were around the centre of the loop. Analyzing the samples using ImageJ software, a curve resembling to the normal distribution was produced (Figure 4 (c)). Thus, the result was consistent the earlier claim that more nanofibres were accumulated at the centre compared to the edges of the deposition area.



Figure 3: (a) Bending instability from previous studies and (b) expected surface topography of the sample

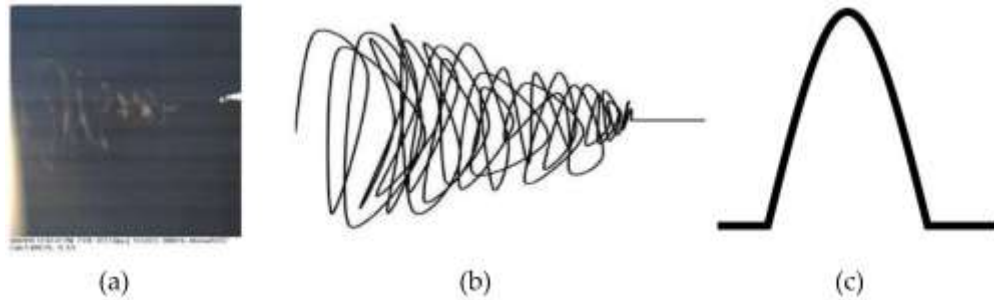


Figure 4: Bending instability through (a) high speed camera, (b) schematic diagram and (c) expected surface topography of the sample

All samples were weighed to obtain the amount of deposited nanofibres. A plot of fibre masses against deposition time was shown in Figure 5. Overall, the results show that the amount of deposited nanofibres increased with respect to deposition time. However, at early deposition time (below 200 seconds), the measured data were observed to fluctuate. This inconsistency might be due to the fact that the calculated standard deviation of the substrate mass was high ( $\pm 0.00537$  g) compared to the actual mass of the deposited nanofibres (0.02-0.03 g). A line of best fit was drawn, and the result suggest that 95% of the measured data were in agreement with the fitted line. The trend of the current results corroborates the ideas of the previous study by Stanger et al. [15] which concluded that for a given set of parameters, the mass of the deposited nanofibres was proportional to the deposition times. It is also worth to note that the y-intercept when  $t = 0$  was not equal to zero. Stanger et al. [15] reported that this could be due to the residual electrostatic charge in the fibres that could be affecting the balance readings.

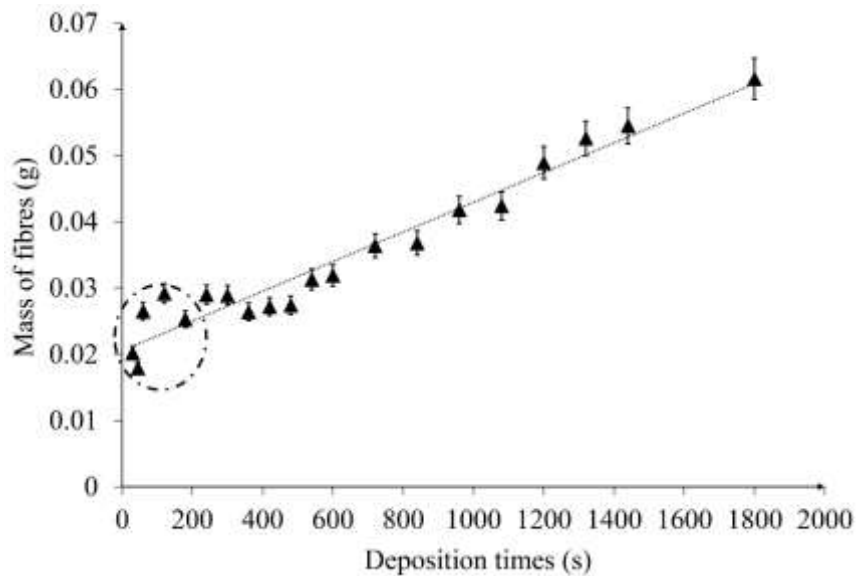


Figure 5: Mass of fibres as a function of deposition time with respective coefficient of determination ( $R^2 = 0.95$ )



From the scanned images, the maximum values of the 3D profiles were used to plot a graph of intensity value as a function of deposition time (Figure 6). Similar to the weighing technique, the intensity value was observed to be increased as the deposition time increased. At early deposition time, the increment of the intensity value was observed to be linear. However, as the value exceeding 200, the curve flattens before reaching a maximum value of 255. This happened due to the limitation owned by the grayscale shades available for an 8-bit greyscale image. The baseline of the graph was found to be around 50 due to the greyscale value of the substrates.

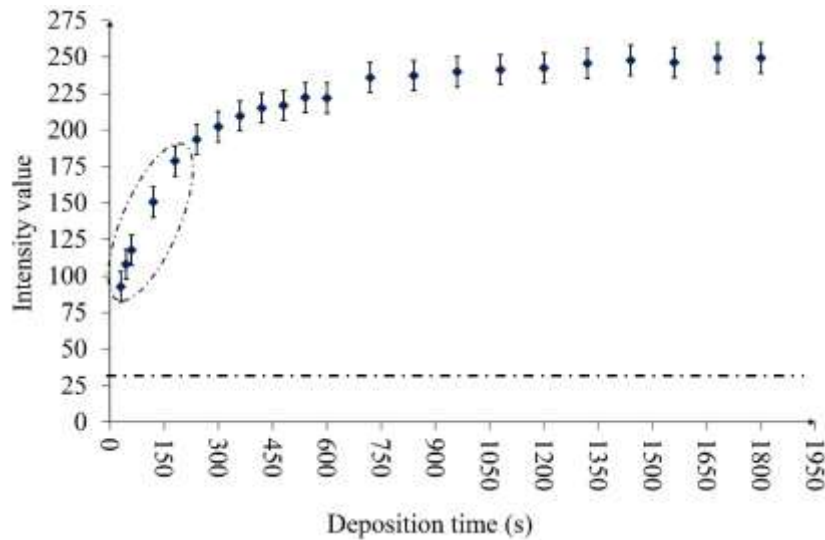


Figure 6: Greyscale intensity with respect to the deposition time

Figure 7 presented the comparison between image analysis and weighing technique at early deposition time (below 200 seconds). Linear regression analysis was used to interpret the data obtained from the comparison. From the figure, the plot presented a strong positive linear correlation between greyscale intensity and deposition time. In addition, a strong evidence of image analysis technique was found when 98.9% of the coefficient determination ( $R^2$ ) fitted the best line compared to only 36.4% for weighing technique. By comparing the two results, 98.9% of the image analysis values explain the variability of the data around its mean compared to the only 36.4% for weighing technique. Further statistical tests were done using P-values to investigate the significance between the data obtained with the deposition times. In this case, the null hypothesis is that there is no significant difference between the sample mean of greyscale intensity and mass of fibres. P-values showed that image analysis data have a greater evidence against the null hypothesis since the p-values obtained is less than 0.005 compared to p-value of the weighing data (p-value 0.282). Thus, it is safe to say that, at early deposition times, the fitted model of image analysis was in better agreement when comparing to the data produced by weighing technique. An encouraging finding was found when using the Pearson correlation coefficient for measuring the relationship between dependent and independent variables for both methods where r value for image analysis is higher compared to the weighing technique with 0.99431 and 0.01401 respectively.

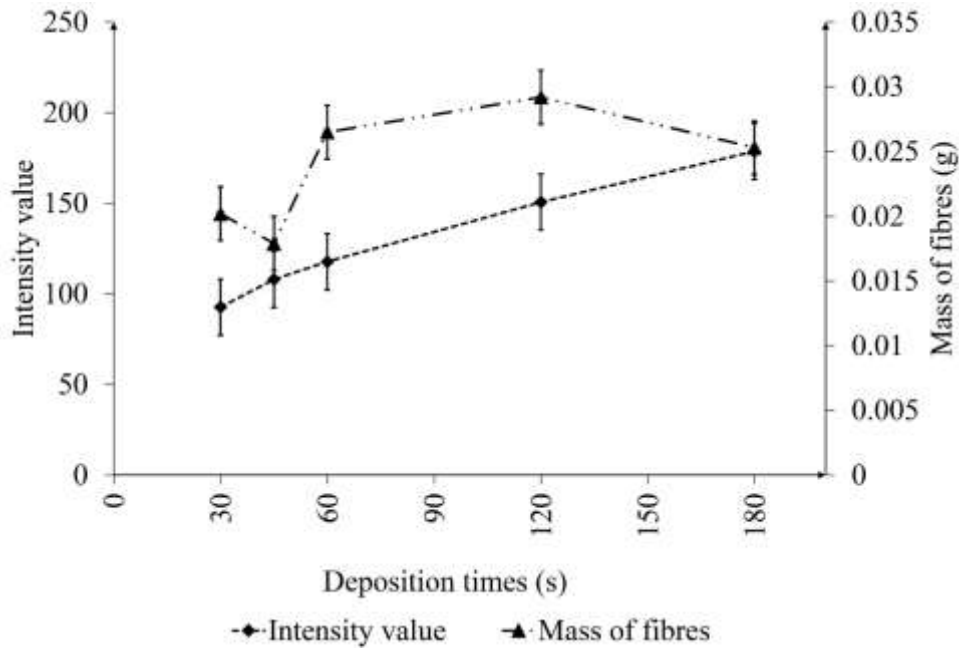


Figure 7: A comparison between image analysis and weighing technique at short deposition times of 30 to 180s

The data was further supported with t-test values to find the stronger evidence between both techniques. The results showed that 16.167 represent the image analysis technique while 1.30 represent for weighing technique. The greater the magnitude of t-test, the greater evidence against the null hypothesis, thus indicating that there was a significant relationship between greyscale intensity and the deposition time.

From SEM micrograph, uniform and randomly oriented polyvinyl alcohol electrospun nanofibres were observed (Figure 8). The fibre diameters of the electrospun nanofibres were measured from 100 different locations with the average of 231.71 nm ( $\pm 17.15$  nm) as depicted in Figure 9. The uniform electrospun nanofibres obtained proved that the used of paper substrates did not influence the formation, thinning and solidifying process of the electrospun nanofibres.



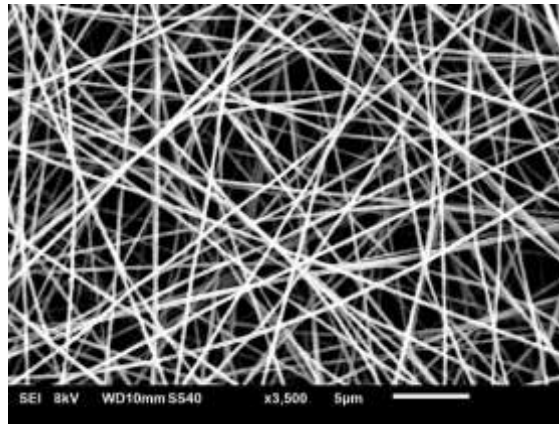


Figure 8: A typical SEM micrograph of poly(vinyl alcohol) electrospun nanofibres

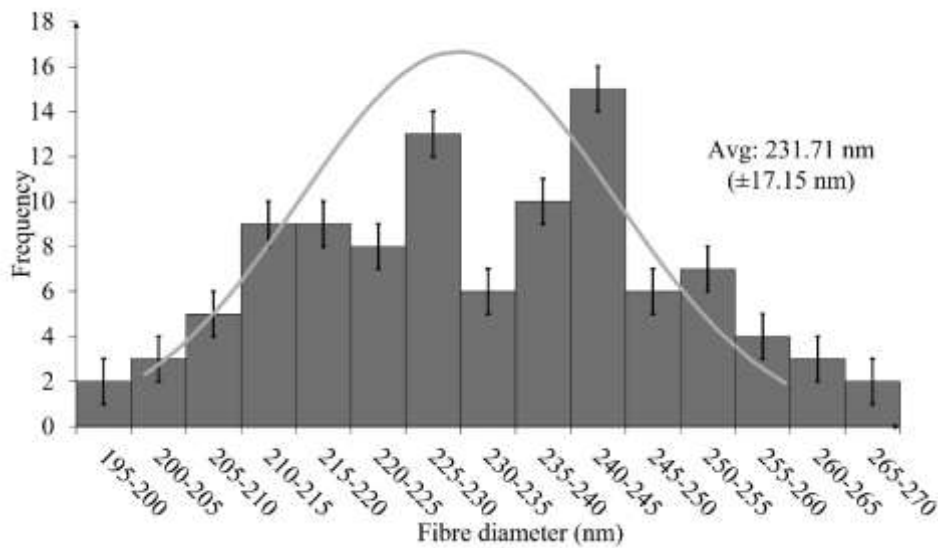


Figure 9: Fibre diameter distribution of the electrospun nanofibres

#### 4.0 CONCLUSION

The experiment was undertaken to compare image analysis and weighing technique for predicting the amount of deposited electrospun nanofibres. In general, it seems that both weighing and image analysis techniques were capable of showing the increasing amount of deposited nanofibres with respect to the collection times. However, a direct comparison between these techniques confirmed that greyscale image analysis technique was superior during short collection times. The findings further support a statistical analysis which showed a strong correlation between greyscale intensities and deposition times compared to a weaker correlation when using weighing technique. The uniform electrospun nanofibres produced from the experiment showed that the used of papers as substrates did not influence the formation of the electrospun nanofibres. Taken together, these findings extend the knowledge of a new non-destructive technique for

predicting the amount of deposited electrospun fibres especially for a small amount of deposited electrospun nanofibres. In addition, this developed technique has the potential to be used as an automated online quality control within manufacturing of electrospun nanofibres.

## ACKNOWLEDGMENTS

This work fully supported by the Ministry of Higher Education Malaysia through the Fundamental Research Grant Scheme FRGS/2/2014/TK01/FKM/02/F00233. Special thanks to the members of Advanced Materials Characteristics Lab (AMCHAL), Centre for Advanced Research on Energy (CARE) and the Faculty of Mechanical Engineering, Universiti Teknikal Malaysia Melaka (UTeM) for their continuous support for this project.

## REFERENCES

- [1] Z. M. Huang, Y. Z. Zhang, M. Kotaki and S. Ramakrishna, "A review on polymer nanofibers by electrospinning and their applications in nanocomposites," *Composites Science and Technology*, vol. 63, no.15, pp. 2223–2253, 2003.
- [2] W. E. Teo and S. Ramakrishna, "A review on electrospinning design and nanofibre assemblies," *Nanotechnology*, vol. 17, no. 14, pp. 89–106, 2006.
- [3] I. S. Chronakis, "Novel nanocomposites and nanoceramics based on polymer nanofibers using electrospinning process - A review," *Journal of Materials Processing and Technology*, vol. 167, no. 2-3, pp. 283–293, 2005.
- [4] D. H. Reneker and A. L. Yarin, "Electrospinning jets and polymer nanofibers," *Polymer*, vol. 49, no. 10, pp. 2387–2425, 2008.
- [5] G. Taylor, "Disintegration of water drops in an electric field," *Royal Society a Mathematical, Physical and Engineering Sciences*, vol. 280, no. 1382, pp. 383–397, 1964.
- [6] C. Zhang, X. Yuan, L. Wu, Y. Han and J. Sheng, "Study on morphology of electrospun poly(vinyl alcohol) mats," *European Polymer Journal*, vol. 41, no. 3, pp. 423–432, 2005.
- [7] D. H. Reneker, A. L. Yarin, H. Fong and S. Koombhongse, "Bending instability of electrically charged liquid jets of polymer solutions in electrospinning," *Journal of Applied Physics*, vol. 87, no. 2000, pp. 4531–4547, 2000.
- [8] S. Ramakrishna, K. Fujihara, W. E. Teo, T. Yong, Z. Ma and R. Ramaseshan, "Electrospun nanofibers: Solving global issues," *Materials Today*, vol. 9, no. 3, pp. 40–50, 2006.
- [9] N. A. Munajat, A. H. Nurfaizey, A. A. M. Bahar, K. Y. You, S. H. S. M. Fadzullah and G. Omar, "High-frequency dielectric analysis of carbon nanofibers from pan precursor at different pyrolysis temperatures," *Microwave and Optical Technology Letters*, vol. 60, no. 9, pp. 2198-2204, 2018.
- [10] A. H. Nurfaizey, N. Tucker, J. Stanger and M. P. Staiger, "Functional nanofibres in clothing for protection against chemical and biological hazards," in *Functional Nanofibers and Their Applications*, Q. Wei. Cambridge: Woodhead Publishing Limited, 2012, pp. 236–261.

- [11] H. Matsumoto and A. Tanioka, "Functionality in electrospun nanofibrous membranes based on fiber's size, surface area, and molecular orientation," *Membranes*, vol. 1, no. 3, pp. 249–264, 2011.
- [12] D. Aussawasathien, C. Teerawattananon and A. Vongachariya, "Separation of micron to sub-micron particles from water: Electrospun nylon-6 nanofibrous membranes as pre-filters," *Journal of Membrane Science*, vol. 315, no. 1, pp. 11–19, 2008.
- [13] R. S. Barhate, C. K. Loong and S. Ramakrishna, "Preparation and characterization of nanofibrous filtering media," *Journal of Membrane Science*, vol. 283, no. 1–2, pp. 209–218, 2006.
- [14] N. D. N. Affandi, Y. B. Truong, I. L. Kyratzis, R. Padhye and L. Arnold, "A non-destructive method for thickness measurement of thin electrospun membranes using white light profilometry," *Journal of Materials Science*, vol. 45, no. 5, pp. 1411–1418, 2010.
- [15] J. Stanger, N. Tucker, S. Fullick, M. Sellier and M. P. Staiger, "Insights into the power law relationships that describe mass deposition rates during electrospinning," *Journal of Materials Science*, vol. 47, no. 3, pp. 1113–1118, 2012.
- [16] M. Ziabari, V. Mottaghitalab, S. T. McGovern and A. K. Haghi, "A new image analysis based method for measuring electrospun nanofiber diameter," *Nanoscale Research Letters*, vol. 2, no. 12, pp. 597–600, 2007.
- [17] M. Ziabari, V. Mottaghitalab, S. T. McGovern and K. Haghi, "Measuring electrospun nanofibre diameter: a novel approach," *Chinese Physics Letters*, vol. 25, no. 8, pp. 3071–3074, 2008.
- [18] L. Ghasemi-Mobarakeh, D. Semnani and M. Morshed, "A novel method for porosity measurement of various surface layers of nanofibres mat using image analysis for tissue engineering applications," *Journal of Applied Polymer Science*, vol. 106, no. 4, pp. 2536–2542, 2007.
- [19] W. Sambaer, "The use of novel digital images analysis technique and rheology to characterize nanofiber nonwovens," *Polymer Testing*, vol. 29, no. 1, pp. 82–94, 2010.
- [20] J. J. Stanger, N. Tucker, N. Buunk and Y. B. Truong, "A comparison of automated and manual techniques for measurement of electrospun fibre diameter," *Polymer Testing*, vol. 40, no. 1, pp. 4–12, 2014.
- [21] J. Lee, Y. H. Jeong and D.-W. Cho, "Fabrication of nanofibrous mats with uniform thickness and fiber density," *Macromolecular Materials and Engineering*, vol. 299, no. 9, pp. 1052–1061, 2014.